

A study of the Rössler system

Radford Mitchell, Jr.*

School of Physics

Jawja Institute of Technology,

Atlanta, GA 30332-0430, U.S.A

(Dated: August 25, 2007)

Abstract

In order to become familiar with the tools provided by the periodic orbit theory, we investigate the dynamics of the Rössler ODEs. Using symbolic dynamics and kneading theory the allowed periodic orbits are determined. Next, the inverse topological zeta function is constructed and from this the topological entropy is found. Finally, the leading Lyapunov exponent is calculated, which serves to quantify the chaotic behaviour of the system.

*Electronic address: gtg348v@mail.gatech.edu

Georgia Tech PHYS 7224:
CHAOS, AND WHAT TO DO ABOUT IT
course project, spring semester 2005

I. INTRODUCTION

The periodic orbit theory of classical chaos is an invaluable tool for examining aspects of the behavior of chaotic dynamical systems. The theory expresses all long time averages over chaotic dynamics in terms of cycle expansions [1]. Sums over periodic orbits (cycles) are ordered hierarchically according to the orbit length. If the symbolic dynamics is known and the flow is hyperbolic longer cycles are shadowed by the shorter ones, and cycle expansions converge exponentially or even super-exponentially with the cycle length [6].

In sect. II I derive my differential equation which governs the evolution of the flow in time. The details of my numerical implementation of the method are discussed in sect. III A. In sect. III B, I test the method on the Rössler flow. My results are summarized discuss possible improvements of the method in sect. V. Why I failed to complete the project is explained in Appendix A.

II. MY PROBLEM DEFINED

A periodic orbit is a solution (x, T) , $x \in \mathbb{R}^d$, $T \in \mathbb{R}$ of the *periodic orbit condition*

$$f^T(x) = x, \quad T > 0 \tag{1}$$

for a given flow or discrete time mapping $x \mapsto f^t(x)$. Our goal is to determine periodic orbits of flows defined by first order ODEs

$$\frac{dx}{dt} = v(x), \quad x \in \mathcal{M} \subset \mathbb{R}^d, \quad (x, v) \in \mathbf{T}\mathcal{M} \tag{2}$$

in d dimensions. Here \mathcal{M} is the phase space (or state space) in which evolution takes place, and the vector field $v(x)$ is smooth (sufficiently differentiable) almost everywhere.

A. My Equations

For the Rössler flow, $x \in \mathbb{R}^3$ and is determined by the vector field $v(x)$ given by

$$\begin{aligned}
\dot{x} &= -y - z \\
\dot{y} &= x + ay \\
\dot{z} &= b + z(x - c)
\end{aligned}
\tag{3}$$

In this particular version of the Rössler flow, we choose $a = b = 0.2$ and $c = 5.7$. The divergence of the flow is given by $\nabla \cdot v(x) = \frac{\partial \dot{x}}{\partial x} + \frac{\partial \dot{y}}{\partial y} + \frac{\partial \dot{z}}{\partial z} = a + x - c$. Clearly the flow is not conservative, and, furthermore, the contraction/expansion of volumes is not uniform in the phase space.

There are two fixed points of the system

$$p^\pm = \frac{c \pm \sqrt{c^2 - 4ab}}{2a}(a, -1, 1)
\tag{4}$$

For our particular choice of parameters the two equilibrium points are $p^+ = (5.692973, -28.464869, 28.464869)$ and $p^- = (0.007026, -0.035131, 0.035131)$. The linearized stability exponents of these fixed points are $(\lambda_1^+, \lambda_2^+) = (0.1929, -4.596 \times 10^{-6} \pm i5.428)$ and $(\lambda_1^-, \lambda_2^-) = (-5.686, 0.0970 \pm i0.9951)$ [1]. This means that trajectories which start near the fixed point located far from the origin rotate and are *slowly* attracted to the stable eigenplane, while at the same time move away along the direction of the unstable eigenvector. Trajectories originating near p^- also rotate and move away along the unstable direction but the attraction to the stable manifold in this case is quite extreme ($\Lambda_z \approx 10^{-15.6}$) [1].

It proves convenient to reduce the three dimensional flow to a one dimensional map using a return map. First, one creates a Poincaré section of the flow at a particular value of θ_0 , which are the set of points

$$\Omega = \{(r, \theta, z) \mid r > 0, \theta = \theta_0\}.
\tag{5}$$

The flow is then reduced to a map via the function f_Ω given by:

$$r_{n+1} = f_\Omega(r_n) \equiv \phi^\tau(r_n), \quad r_n, r_{n+1} \in \Omega
\tag{6}$$

Here ϕ denotes the Poincaré map and τ the return time, which varies for each iteration of the map. In practice these return maps were obtained by recording ~ 3000 traversals of the section by an arbitrary trajectory and discarding the first ~ 500 or so data points in order to allow the flow sufficient time to settle onto the attractor.

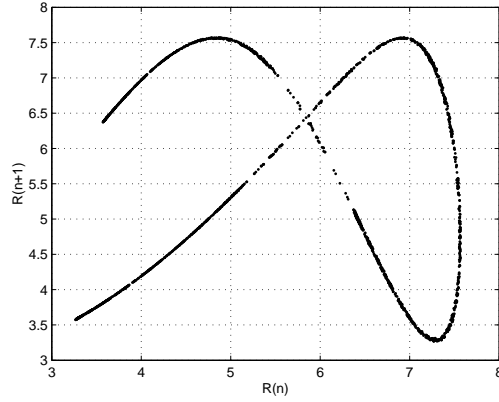


FIG. 1: Return map: $R(n+1)$ versus $R(n)$ for a section taken at $\theta_0 = 30$

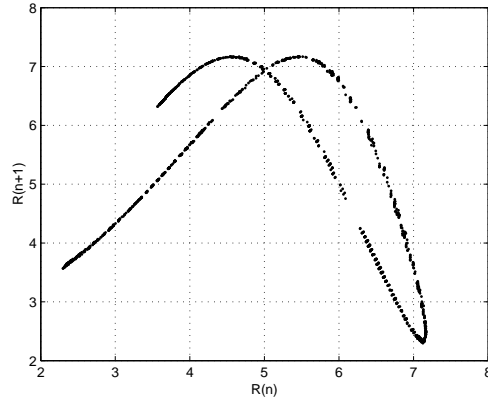


FIG. 2: Return map: $R(n+1)$ versus $R(n)$ for a section taken at $\theta_0 = 50$

Denote by δ_n the deviation of a point x_n on the periodic orbit p from the nearby point y_n ,

$$x_n = y_n + \delta_n.$$

Let $x(t) = f^t(x)$ be the state of the system at time t obtained by integrating (2), and $J(x, t) = dx(t)/dx(0)$ be the corresponding Jacobian matrix obtained by integrating

$$\frac{dJ}{dt} = AJ, \quad A_{ij} = \frac{\partial v_i}{\partial x_j}, \quad \text{with } J(x, 0) = \mathbf{1}. \quad (7)$$

For the Rössler flow,

$$A = \begin{pmatrix} 0 & -1 & -1 \\ 1 & a & 0 \\ z & 0 & x - c \end{pmatrix}$$

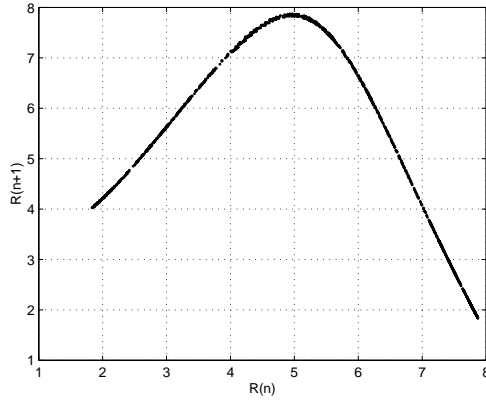


FIG. 3: Return map: $R(n+1)$ versus $R(n)$ for a section taken at $\theta_0 = 95$

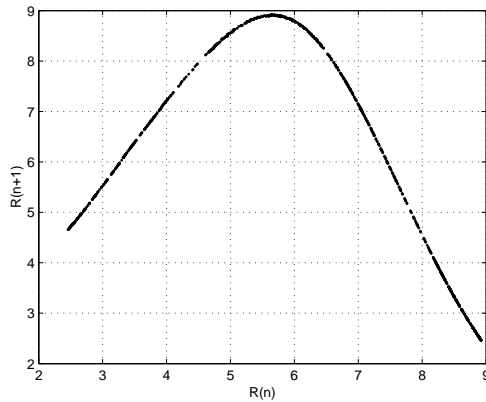


FIG. 4: Return map: $R(n+1)$ versus $R(n)$ for a section taken at $\theta_0 = 140$

B. Symbolic Dynamics

Once the generic behavior of the flow has been determined, one may partition the phase space into various regions, labeling each one with its own unique symbol. So, in general, one is dealing with some finite set $\{1, 2, \dots, n\}$ of symbols, which is known as the *alphabet* or *state set*. Two distinct sequence spaces can be formed from this set. The one-sided space is $\{1, 2, \dots, n\}^{\mathbb{N}}$ whose sequences are of the form $(s_0 s_1 s_2 \dots)$. The two-sided sequence space is $\{1, 2, \dots, n\}^{\mathbb{Z}}$ and these sequences are of the form $(\dots s_{-2} s_{-1} s_0 s_1 s_2 \dots)$. In both cases each $s_i \in \{1, 2, \dots, n\}$ [3].

For the Rössler flow, the return maps of interest are unimodal on some interval, I , of the radial coordinate. Thus, the most logical partitioning of the phase space is whether a given

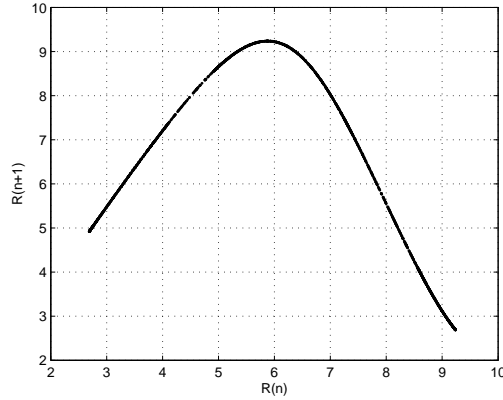


FIG. 5: Return map: $R(n+1)$ versus $R(n)$ for a section taken at $\theta_0 = 215$

trajectory falls to the right or to the left of the critical point (x_c). If $x_i < x_c$, then $s_i = 0$, and if $x_i > x_c$, then $s_i = 1$ (we denote this one-sided sequence space Σ_2). This sequence space can be defined as a metric space by introducing the notion of a “distance” between two sequences, $S = (s_0 s_1 s_2 \dots)$ and $T = (t_0 t_1 t_2 \dots)$ given by $d[S, T] = \sum_{i=0}^{\infty} \frac{|s_i - t_i|}{2^i}$, which is a convergent series. This metric allows us to determine how “close” two sequences are to one another.

Next, we define the shift transformation on this space. The shift map $\sigma : \Sigma_2 \mapsto \Sigma_2$ is given by $\sigma(s_0 s_1 s_2 s_3 \dots) = (s_1 s_2 s_3 \dots)$. One can see why it is called the shift map as it discards the first entry and shifts all subsequent entries one place to the left. Clearly, σ is a two-to-one map on Σ_2 . Furthermore, in the metric space defined above, σ is a continuous map [2].

Periodic points in Σ_2 have the property that $\sigma^p(x) = x$. For $p > 0$, if p is the least such power that satisfies the preceding equation, we say that x has *period* p . The number of periodic points is countably infinite and they are dense in the space [3]. Eventually periodic points have the property that $\sigma^k(x) = \sigma^{k+p}(x)$.

For $x \in I$, its itinerary is given by $S(x) = s_0 s_1 s_2 \dots$. This encoding of the itinerary via S gives an equivalence between the dynamics of the return map, $f_\Omega : I \mapsto I$, and the shift map, $\sigma : \Sigma_2 \mapsto \Sigma_2$. $S : I \mapsto \Sigma_2$ is known as a homeomorphism and $S(f_\Omega(x)) = \sigma(S(x))$. This implies that the maps σ and f_Ω are topologically conjugate to one another (i.e., they are completely equivalent in terms of their dynamics) [2].

C. Kneading Theory

First, we must determine an ordering for our sequence space. This is achieved by associating a binary number τ with each itinerary, $S(x) = s_1s_2s_3\dots$, in our space via the following algorithm:

$$w_1 = s_1$$

$$w_{t+1} = \begin{cases} w_t & \text{if } s_{t+1} = 0 \\ 1 - w_t & \text{if } s_{t+1} = 1 \end{cases} \quad (8)$$

Note that this is slightly modified from [1]. The binary number τ is then given by:

$$\tau = 0.w_1w_2w_3\dots = \sum_{t=1}^{\infty} \frac{w_t}{2^t} \quad (9)$$

Now that our space is well-ordered, we must determine a boundary with respect to this ordering between admissible and inadmissible itineraries. The itinerary of the critical point, $S(f_{\Omega}(x_c))$, of our unimodular return map (commonly referred to as the *kneading sequence*) defines the boundary. The kneading value $K = \tau(x_c)$ given by (9) is the largest value that any admissible sequence can have. Any sequence S has some maximum value τ^{max} for its corresponding binary number and is given by

$$\tau^{max}(S) = \sup_k \tau(\sigma^k S) \quad (10)$$

The orbit S is admissible if and only if $\tau^{max}(S) \leq K$ [7]. In practice, however, the ideas presented in [2] are used to determine the allowed orbits and this is summarized in sect. III B.

III. IMPLEMENTATION OF MY METHOD

A. Numerical implementation

A fourth order Rünge-Kutta scheme was used to advance the trajectory forward in time using Cartesian coordinates. When the trajectory begins to near θ_0 (the location of the Poincaré section), the program checks to see when it crosses the section. Once this happens, “Hénon’s trick” is employed in *cylindrical* coordinates so that the trajectory lands exactly

on the section. Essentially this involves switching dt with $d\theta$ and using $|\theta - \theta_0|$ as the “time-step”, where θ is understood to be the angular position of the previous time step. Converting $v(x)$ to cylindrical coordinates yields:

$$\begin{aligned}\dot{r} &= -z \cos \theta + ar \sin^2 \theta \equiv f_1(r, \theta, z) \\ \dot{\theta} &= 1 + \frac{z}{r} \sin \theta + a \sin \theta \cos \theta \equiv f_2(r, \theta, z) \\ \dot{z} &= b + z(r \cos \theta - c) \equiv f_3(r, \theta, z).\end{aligned}\tag{11}$$

and using the chain rule, one obtains the new set of equations that are to be integrated in θ

$$\begin{aligned}\frac{dr}{d\theta} &= f_1(r, \theta, z)/f_2(r, \theta, z) \\ \frac{dt}{d\theta} &= 1/f_2(r, \theta, z) \\ \frac{dz}{d\theta} &= f_3(r, \theta, z)/f_2(r, \theta, z).\end{aligned}\tag{12}$$

Once the trajectory has landed on the section t and θ are again switched and the new coordinate values are converted back to Cartesian [4].

B. Initialization of the search

For our particular analysis, we chose $\theta_0 = 230^\circ$ as the location in the xy -plane for the Poincaré section. The return map for this section was constructed and from this an estimate for the critical point was obtained and its z -value was recorded. Using this information, the kneading sequence was examined as a function of the time step Δt . It was found to converge to $S(x_c) = 10010111111010110110010110101\dots$ giving $\tau_c = .111001010101100100100011011001\dots$ for its kneading value defined by (9).

Consider the sequence $T = t_1 t_2 t_3 \dots$ and let n be the first entry where $S(x_c) = s_1 s_2 s_3 \dots$ and T differ. As Devaney does in [2], we define an ordering \prec on the sequence space Σ_2 inductively. Let $\gamma = \sum_{k=1}^{n-1} t_k$; if γ is even and $t_n < s_n$ or if γ is odd and $t_n > s_n$, then $T \prec S(x_c)$ and the sequence is an admissible one. If neither condition is satisfied, then we prune this orbit. This is how the admissibility of orbits was determined in practice.

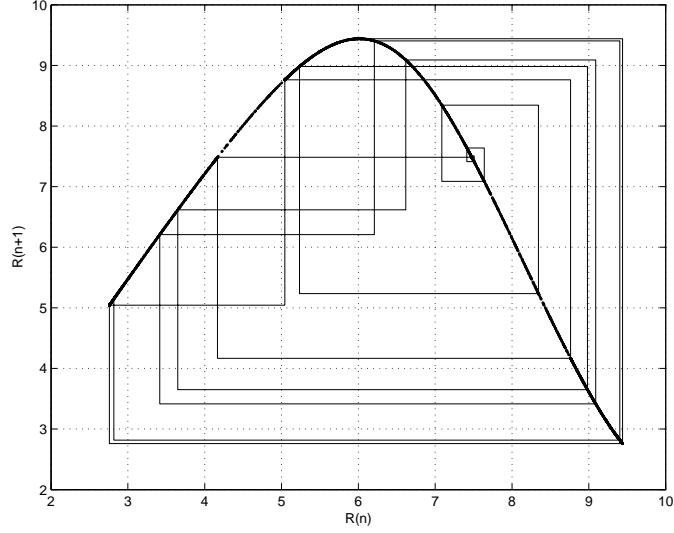


FIG. 6: The first 22 iterates of the kneading sequence

n_p	1	2	3	4	5	6	7	8	9
	1	01	001	0111	01011	001011	0101011	01011011	010110111
			011		01111	010111	0110111	01010111	010101111
						011111	0101111	01101111	011011111
							0111111	00101111	011010111
								01011111	001011011
								01111111	011101111
								00101101	010111111
									001001011
									011111111
									010101011

TABLE I: Admissible itineraries for periodic orbits up to length 9

Using the results from Appendix E in [1] for unimodal maps, we have that the inverse topological zeta function is given by the following polynomial:

$$1/\zeta_{top}(z) = \prod_p (1 - z_p^n) = (1 - z) \sum_{i=0}^{n-1} a_i z^i;$$

$$a_i = \prod_{j=1}^i (-1)^{s_j}, a_0 = 1 \quad (13)$$

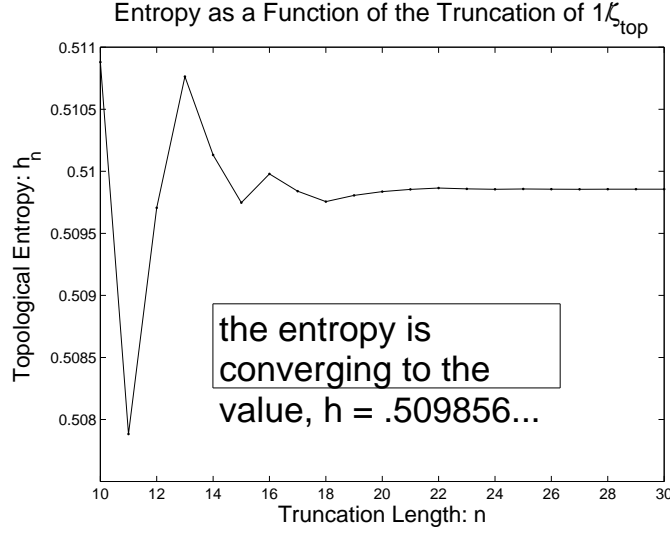


FIG. 7: Topological entropy as a function of the truncation of the inverse zeta function

Here the s_j are the entries in the kneading sequence $S = s_1 s_2 s_3 \dots$. Since we have not been able to determine whether the kneading sequence is periodic, eventually periodic, or aperiodic, n can be either finite or infinite. This ambiguity should not pose a problem, however, since we will eventually have to truncate the expanded inverse zeta function anyway. For our particular kneading sequence, $S(f_\Omega(x_c))$, we have the following inverse topological zeta function, which we have truncated to the first 31 terms:

$$1/\zeta_{top}(z) = (1 - z)(1 - z - z^2 - z^3 + z^4 + z^5 - z^6 + z^7 - z^8 + z^9 - z^{10} + z^{11} - z^{12} - z^{13} + z^{14} + z^{15} - z^{16} + z^{17} + z^{18} - z^{19} - z^{20} - z^{21} - z^{22} + z^{23} + z^{24} - z^{25} + z^{26} + z^{27} - z^{28} - z^{29} + z^{30}) \quad (14)$$

IV. THE HOUR OF TRIUMPH

...unfortunately has not come yet.

V. DISCUSSION

Ultimate goals of the project were to find the periodic orbits using the Newton-Raphson algorithm in conjunction with the multiple-shooting method. Time-evolving the Jacobian along these trajectories would have allowed me to compute the stability for each of the orbits, which, in turn, would have given an estimate for the leading Lyapunov exponent. However, I did attain the minimal goal of computing return maps, finding the kneading sequence (for my chosen parameters), pruning orbits, constructing a topological zeta function, and evaluating the topological entropy in terms of the truncation of this function.

My main result was determining a convergent value for the topological entropy of the flow. This result was obtained using the kneading theory associated with unimodal maps. The method is applicable to any map which satisfies the unimodal conditions.

Acknowledgments

I would like to thank Dan Benjamin for his help in formatting TABLE I.

APPENDIX A

I encountered several technical difficulties in trying to use the PCs available on campus. Much time was wasted in compiling the tex file on zero (as acme does not have Latex as far as i was able to ascertain), then scp'ing the ps file to acme, and finally opening the file using the Ghostview on the PC just to see each change that i attempted to make. People tried to help me set up an x-server through zero so that i might be able to use ghostview inside that remote host (with no success), but in the end i was told that i should just buy my own computer - something i intend to do very soon. Much of this is my fault, as i had grown quite used to the Sun workstations at my old school; instead, i should have taken my previously abundant spare time and familiarized myself with the various operating systems that are out there.

More than anything, though, the use of MATLAB as a programming language was my biggest mistake. This semester turned out to be a lot more work than i had anticipated

and i frequently turned to MATLAB, since i knew i at least had access to it in the library, for help on the homework problems. One week led to another and before i knew it i was using an unfamiliar (as well as EXTREMELY slow) language to do my project. Now that i have a LINUX account (and more time), i plan to spend some time converting my code to FORTRAN and continue the project.

- [1] P. Cvitanović et al., *Chaos: Classical and Quantum*, advanced graduate e-textbook, available online at ChaosBook.org (Niels Bohr Institute, Copenhagen, 2003).
- [2] R. Devaney, *An Introduction to Chaotic Dynamical Systems*, (The Benjamin/Cummings Publishing Co., Inc., Menlo Park, 1986).
- [3] B.P. Kitchens, *Symbolic Dynamics: One-sided, Two-sided and Countable State Markov Shifts*, (Springer Press, Berlin, 1998).
- [4] H. Bai-Lin, *Elementary Symbolic Dynamics and Chaos in Dissipative Systems*, (World Scientific Publishing Co., Singapore, 1989).
- [5] B. Branner and P. Hjorth, eds., *Real and Complex Dynamical Systems*, (Kluwer Academic Publishers, Dordrecht, 1995).
- [6] H.H. Rugh, “The Correlation Spectrum for Hyperbolic Analytical Maps,” *Nonlinearity* **5** (1992) 1237.
- [7] K.T. Hansen, “Symbolic Dynamics in Chaotic Systems,” Ph.D. Thesis, University of Oslo (1993).